

Theory of far-infrared absorption in small-metal-particle—insulator composites

W. A. Curtin and N. W. Ashcroft

Laboratory of Atomic and Solid State Physics and Materials Science Center, Cornell University, Ithaca, New York 14853

(Received 26 October 1984)

We present a theory of the far-infrared absorption coefficient for metal—alkali-halide composites assumed to consist of finite metal-particle-cluster subcomposites, a geometry very likely to exist in such systems. Three different models for the cluster composite topology are considered: highly metallic clusters, clusters with near-percolation paths of metal, and clusters with weakly allowed tunneling between isolated metallic constituents. For each, the effective dielectric properties of the cluster are first derived and the effective dielectric function for the entire composite is then determined from an application of classical magnetic or electric dipole theory. Subsequent calculations of the absorption coefficient are in reasonable agreement with a number of experimentally observed absorption features, and thus resolve the long-standing discrepancy of orders-of-magnitude difference between theory and experiment in such systems.

I. INTRODUCTION

Because of their applications in technology the electromagnetic properties of metal-insulator composites continue to be of great interest. Many experimental studies of the far-infrared (FIR) absorption in metal—alkali-halide systems have shown unusual results.^{1,2} In particular, the measured FIR absorption coefficients are orders of magnitude larger than those predicted by classical dipolar electromagnetic theories.³ Additional features of the measured absorption in the dilute metal limit are a linear dependence on the volume fraction of metal, a roughly quadratic frequency dependence at low frequencies, but a weak dependence on the size of the particles of the metallic constituent. In the dilute limit, classical theories treat these particles as isolated spheres and yield absorption coefficients smaller by factors of 10^{-1} – 10^{-7} than measured.² Single-particle theories involving phonon excitation at particle surfaces,⁴ nonlocal dielectric response of the small spheres,⁵ particles coated by absorbing oxides,⁶ and the inclusion of quantum size effects,⁷ have all failed to produce sufficiently large absorption coefficients. Theories of particle clustering have largely concentrated on needlelike clusters of particles (or particles coated by absorbing oxides) modeled by ellipsoids.^{8,9} These cluster theories are able to predict large absorption coefficients but only under the assumptions of the existence of absorbing oxide coatings and of major-to-minor axial ratios approaching unreasonably high values of 30:1.

In this paper we present three models for FIR absorption in metal—alkali-halide composites, all of which are based on a view of the composite as a collection of compact, finite-sized metal-cluster *subcomposites*. For each, the calculated absorption coefficients agree well in magnitude and in other features with the most recent experimental results. In the remainder of this section we will discuss the general view of the composite from which all three of our models evolve and briefly discuss the newest experimental findings which provide motivation and justification for the validity of our cluster models. In Secs.

II–IV we present each of our cluster models and their contributions to FIR absorption in detail. In Sec. V we discuss the links between the models, further connections with experimental results, and directions for further study.

Experiments by Carr, Garland, and Tanner¹⁰ and more recently by Curtin *et al.*,¹¹ on granular superconducting samples consisting of Sn embedded in KCl or KBr have provided useful information on the nature of the FIR absorption in these heterogeneous systems. First, for both oxide-coated and oxide-free particle samples the absorption at temperatures below the bulk T_c of Sn is observed to be even larger than that above T_c at frequencies larger than the superconducting gap frequency ω_g . However, when Curtin *et al.* subjected the samples to a heat-treatment process in which only the metal component was melted, they observed (i) modest changes in the normal ($T > T_c$) absorption α_n , but (ii) a superconducting absorption α_s that became equal to or less than the normal-state absorption at all measured frequencies. Since similar effects are seen for both oxidized and unoxidized particles, and since the $T < T_c$ absorption is very different from the $T > T_c$ absorption, it is immediately apparent that an absorptive oxide cannot be the cause of the large absorption coefficients usually measured.

The distinct changes in α_n and α_s of the composite samples upon heat treatment provide valuable new insight into the possible structure of this class of composite materials. The essential point is that heat treatment can affect the connectivity between contiguous particles but does not otherwise significantly affect isolated particles. Further, relaxation time and shape changes associated with melting may alter the magnitude of the single-particle absorption in the normal state but they should not affect the frequency dependence or superconducting behavior. A further conclusion, therefore, is that the anomalous absorption is associated with the clustering of particles. This conclusion is also consistent with the recent work of Devaty and Sievers¹² on Ag particles in gelatin which indicated that samples with deliberately ag-

glomerated particles show much stronger absorption than those with isolated ones. Note that in the electrical sense, individual particles in a cluster may be either strongly or weakly coupled to their neighbors, depending on their separation. The melting process presumably alters this separation and hence the coupling between particles. For example, neighboring particles may fuse together or separate even further because of the relief of local strains. Such changes in the local configuration of particles can then lead to selectively different absorption mechanisms, and hence to different α_n and $\Delta\alpha$ upon heating, as is seen to be the case in the samples studied here.

The presence of large fused clusters in the heat-treated samples is revealed by transmission electron microscopy (TEM) micrographs, which show 500–800 Å Sn single crystals embedded in 2000–3000 Å clusters,¹¹ and suggests a general picture of the composite topology in which clusters of metal particles with effective dielectric properties ϵ and μ are distributed evenly throughout the host medium. The cluster dielectric properties ϵ and μ depend upon the details of the cluster topology and such details are assumed to be modified upon melting of the metallic component. Figure 1 is a schematic of this view of the composite with the three possible cluster topologies which we will consider below in calculating FIR absorption. The first, Fig. 1(a) [fused cluster (FC) model], assumes all metal particles in a cluster to be in good metallic contact with their neighbors. This model is taken to be appropri-

ate to the heat-treated composite samples. The second, Fig. 1(b) [cluster percolation (CP) model], permits some of the particles in a cluster to be electrically isolated from their neighbors by nonconducting coatings of impurities or oxide. The third, Fig. 1(c) [cluster tunnel junction (CTJ) model], assumes the metal particles are electrically coupled only via near-neighbor *tunnel junctions*. The CP and CTJ models are presumed appropriate to the unheated samples and the FC model evolves from these by the effect of heat treatment, which allows particles to fuse and thus renders any barriers to conduction ineffective.

We note that the previous considerations of particle clustering have concentrated on very long needlelike clusters modeled by ellipsoids.^{8,9} However, long chains of particles are susceptible to destruction in the composite fabrication process for the samples we discuss whereas the compact clusters considered here are small enough both to reside in the interstitial regions of the KBr host particle matrix and to remain intact on grinding and compression.

II. FUSED CLUSTER MODEL

In this model, regions of the *heat-treated* composite are assumed to consist of isolated metal-particle clusters with particle radii a and characteristic cluster dimensions $R = 2000\text{--}3000$ Å. As a result of the heat treatment, all the metal particles in a cluster are fused with their neighbors. The clusters can thus acquire a highly metallic

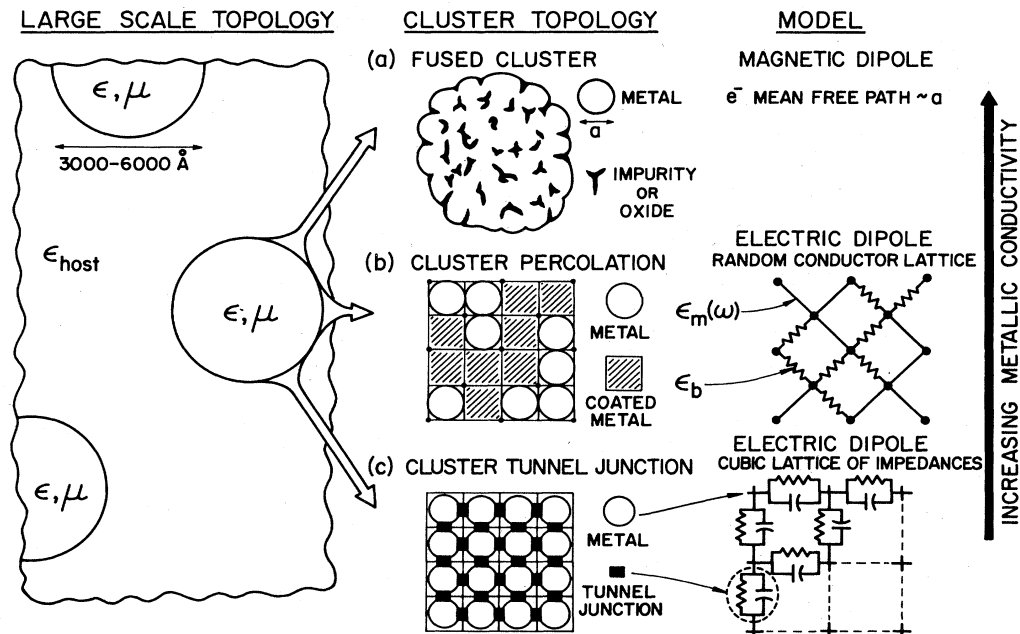


FIG. 1. Composite topology and cluster topologies. The composite consists of isolated clusters. The clusters are modeled in (a) fused cluster model—all metal particles are in good electrical contact with neighbors. Magnetic dipole absorption is large. This model is appropriate to heat-treated composites. (b) Cluster percolation model—only a fraction p of the metal particles can form metallic contacts, the remainder are coated by nonconducting impurities or oxides. Clusters are modeled by networks of conducting and nonconducting bonds. The electric dipole absorption by clusters with p near the percolation threshold is large. This model is appropriate to unheated composites. (c) Cluster tunnel junction model—all metal particles are coated but tunneling between particles is allowed. Clusters are modeled by cubic lattices of tunnel junctions, each junction represented by a resistor and capacitor in parallel. Electric dipole absorption is large for sufficiently small interparticle conductivities. This model is also appropriate to the unheated composites.

character. However, because of impurity (oxide) and void space the metal fill fraction of each cluster is still only approximately that of close random packing and, most importantly, the electronic scattering time τ is dominated by a scattering length determined by the *single-particle dimension* a (i.e., $l \approx a$), rather than by the much larger cluster dimension R . The heat-treated clusters are similar in connectivity to "steel wool" in that they consist of many interconnected paths of metal. At the same time, however, they are not completely metallic in the space-filling sense. In this structure large absorption results from the dissipation of circulating eddy currents in the clusters induced by the applied magnetic field.

The absorption coefficient of a composite containing a dilute collection of magnetically polarizable clusters is easily calculated and has indeed been well studied for the case of homogeneous metallic spheres.^{2,13,14} The magnetic polarizability of a sphere with dielectric function ϵ and radius r is $\gamma_m = 3[3/x^2 - 1 - 3 \cot(x)/x]/8\pi$, where $x = \omega\epsilon^{1/2}r/c$, and the magnetic permeability of the sphere is thus $\mu = (1 + 8\pi\gamma_m/3)/(1 - 4\pi\gamma_m/3)$. The effective permeability μ_{comp} of a composite containing a volume fraction $\eta \ll 1$ of such spheres embedded in a nonmagnetic host of dielectric ϵ_h is analogous to the expression for the two-component Maxwell-Garnett effective dielectric function,¹⁵ i.e.,

$$\mu_{\text{comp}} = 1 + 3\eta \frac{\mu - 1}{\mu + 2}. \quad (2.1)$$

The resulting absorption coefficient is given by $\alpha = 2(\omega/c)\text{Im}(\mu_{\text{comp}}\epsilon_h)^{1/2}$. If $x \ll 1$, then the well-known expansion of γ_m and μ in x leads to

$$\alpha = \frac{\eta}{10c} \left[\frac{\omega r}{c} \right]^2 \epsilon_h^{1/2} \text{Re}\sigma. \quad (2.2)$$

At FIR frequencies and for metalliclike spheres, $\text{Re}\sigma$ is constant in frequency. The magnetic dipole (MD) absorption is therefore quadratic in frequency and increases with the sphere size. As ω increases and x approaches 1, higher-order terms contribute appreciably in the expansion of γ_m , the result being a saturation in α with increasing frequency as the skin depth $c/\omega\epsilon^{1/2}$ becomes smaller than the sphere radius and part of the sphere volume becomes screened from the external field.

Applying the MD theory to fused clusters, the appropriate "sphere size" is the cluster size R , where $R \gg a$. Since we consider the absorption of large, inhomogeneous clusters to all orders in x , our theory differs from that of Ref. 14 and is not subject to the objections raised against Ref. 14. We assume the dielectric constant ϵ is to be describable by a Drude model, with an electronic relaxation time given by $\tau = a/v_f \ll R/v_f$, multiplied by a factor of 0.5 to account for the random-packing fraction of the metal. We then find that the crucial quantity $x = \omega\epsilon^{1/2}R/c$ is much larger than that for an isolated metal particle ($x_{\text{MP}} = \omega\epsilon^{1/2}a/c$); correspondingly this leads to considerably "enhanced" absorption. Note that, as a result of the scattering length $l \approx a$, x is also much smaller than the value expected for a completely metallic cluster ($x_{\text{MC}} = \omega\epsilon^{1/2}R/c$) thus delaying in frequency the onset of the skin-depth induced saturation of α . Al-

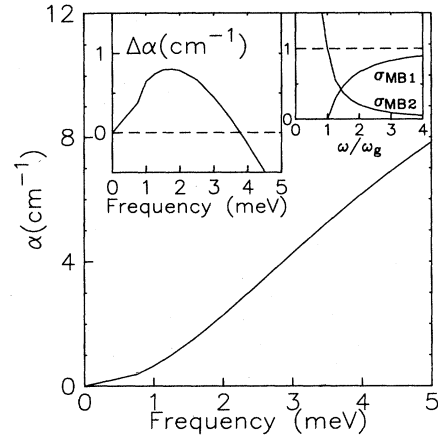


FIG. 2. Absorption coefficient $\alpha(\omega)$ vs frequency for the fused cluster model. The cluster radius is $R=3000 \text{ \AA}$ and the electronic scattering time is $\tau=a/v_f$, $a=250 \text{ \AA}$. The absorption is magnetic dipole in nature but shows marked deviations from quadratic frequency dependence as the frequency-dependent skin depth approaches the cluster radius from above. The agreement with the experimental results of Curtin *et al.* on *heat-treated*, oxide-free samples is quite good. Left inset— $\Delta\alpha = \alpha_n - \alpha_s$ vs frequency. $\Delta\alpha$ is positive just above the gap frequency $\omega_g = 1 \text{ meV}$. Right inset—Mattis-Bardeen form for the real and imaginary parts of the superconducting conductivity, normalized to the real part of the normal-state conductivity, employed to calculate $\Delta\alpha$.

though the absorption coefficient of the fused cluster composite is large, it actually increases with frequency more slowly than ω^2 . Figure 2 shows the magnetic dipole absorption for a composite with total metal fill fraction $f=0.02$ and radius $R=3000 \text{ \AA}$ clusters consisting of Sn with near-random-packing fill fraction equal to 0.65, $a=250 \text{ \AA}$, and $\tau=a/v_f$ embedded in a KBr host ($\epsilon_h=4.84$). The parameters are chosen to agree with those of the oxide-free, *heat-treated* Sn samples studied by Curtin *et al.*, the agreement with the experimental data is extremely good. Similar agreement is also obtained for $R=2000 \text{ \AA}$ clusters, with $\tau=2a/v_f$.

The superconducting absorption of the fused cluster composite has also been calculated and the quantity of interest, $\Delta\alpha = \alpha_{\text{normal}} - \alpha_{\text{super}}$, is shown in the inset of Fig. 2 with $\omega_g = 1 \text{ meV}$. The complex conductivity in the superconducting state is taken to be of the Mattis-Bardeen¹⁶ (MB) form as shown in the second inset of Fig. 2. The predicted $\Delta\alpha$ is in qualitative agreement with the experimental results. Such discrepancies as there are may be a result of the inapplicability of the MB formalism to metal-like clusters of radii $R \geq \xi_0$ where ξ_0 is the superconducting coherence length. The sharp drop in $\Delta\alpha$ above ω_g is physically expected because the superconducting conductivity is smaller than the normal-metal conductivity. Accordingly, the skin depth is larger, implying that more of the cluster is accessible for absorption. The ensuing competition between a decreased ability to absorb and an increased volume for absorption can thus lead to an absorption in the superconducting state comparable to or even exceeding that of the normal state. For isolated

small metal particles, a sharp drop in $\Delta\alpha$ is not expected since the entire particle volume is absorbing in the normal state (i.e., $x \ll 1$) and hence for $T < T_c$ only the effect of the lower conductivity will be observable.

The remarkable agreement between the fused cluster MD absorption theory and the experimental results, both in magnitude and in the frequency dependences of the normal and superconducting absorption, allows us to conclude that the heated samples can indeed be thought of as structures resembling large metallic "steel-wool"-like clusters. If this is the case then it follows that prior to heat treatment the samples must be in the same or at least a very similar geometry, namely they must consist of dispersed clusters of characteristic size $R \approx 2000\text{--}3000$ Å. But, the measured unheat-treated sample absorption coefficients are *not* consistent with the fused cluster MD absorption in frequency dependences of either α or $\Delta\alpha$. We therefore deduce that in the unheat-treated state many of the metal particles in a cluster must be electrically isolated from their neighbors. The CP and CTJ models are consistent with such a topology and for this reason we consider these models and their contributions to FIR absorption next.

III. CLUSTER PERCOLATION MODEL

In the cluster percolation model, the composite is assumed to consist of a dispersion of isolated metal-particle clusters, each on a size scale of a few thousand angstroms. Each cluster is itself a composite consisting of metal particles, voids, and impurities and/or oxide coatings which serve to electrically isolate a certain volume fraction of the metal particles from their neighbors. The remaining metal particles in the cluster, of volume fraction p , are electrically coupled to an extent appropriate for a finite-size system of metal particles of fill fraction p embedded in a nonconducting host. We now observe that if p for a cluster happens to be near a critical fill fraction for percolation, p_c , the unisolated metal particles will form tenuous chains, an extended structure that will be shown to lead to large low-frequency absorption. The calculation of the composite absorption is in two steps. First, the dielectric function $\epsilon(p, \omega) = \epsilon'(p, \omega) + i\epsilon''(p, \omega)$ of a cluster with unisolated metal fill fraction p must be determined. Next, the dielectric function of the entire composite $\epsilon_{\text{comp}}(\omega)$ is calculated by using the multicomponent Maxwell-Garnett effective dielectric function generalized to its continuum form. The components are the clusters described by $\epsilon(p, \omega)$ at a fill fraction $fN(p)dp$ where f is the total metal volume fill fraction and $N(p)$ is the fraction of clusters in the composite with unisolated metal fill fractions between p and $p + dp$. Statistically, we must expect some clusters to have $p \approx p_c$ and hence some "enhanced" absorption. The absorption coefficient is then immediately calculable from $\alpha(\omega) = (2\omega/c)\text{Im}[\epsilon_{\text{comp}}(\omega)]^{1/2}$.

A. Cluster dielectric function

Each cluster or subcomposite is geometrically modeled as a simple cubic lattice with lattice spacing $2a$ and edge length L . Between the sites of the lattice are dielectric bonds assigned a dielectric constant of either $\epsilon_m(\omega)$ or ϵ_b

with the fraction p of $\epsilon_m(\omega)$ bonds corresponding to the volume fraction of unisolated metal particles of dielectric $\epsilon_m(\omega)$ allowed to be electrically coupled. As the fraction p increases from 0 to 1, we expect a transition in the effective cluster dielectric function from ϵ_b to $\epsilon_m(\omega)$ to occur. In analogy to infinite systems, such a transition should occur rather rapidly near a critical $p = p_c$ at which point a continuous line of $\epsilon_m(\omega)$ bonds will be found to extend from one side of the cluster to the other. An actual singularity in $\epsilon(p, \omega)$ of the infinite system would not, however, occur here because of the existence of a nonzero ratio of dielectric components $\epsilon_b/\epsilon_m(\omega)$. Further, for the finite cluster, there is broadening of the transition attributable to the fact that the cluster is not of infinite extent. This size-dependent smearing augments the broadening effect of the nonzero dielectric ratio. For sufficiently small clusters and good metallic components, finite-size effects are likely to dominate this broadening.

For a given configuration of conducting and nonconducting bonds, an effective $\epsilon(p, \omega)$ may be calculated for the model cluster. At fixed p , many configurations are possible, however, and hence an exact calculation of $\epsilon(p, \omega)$ as an average over all configurations is quite lengthy. We wish to avoid such a procedure and can do so by employing a real-space renormalization group (RSRG) technique (discussed in detail in Ref. 17) to calculate $\epsilon(p, \omega)$. For a finite system, the RSRG transformation, which reduces the number of bonds along a cube edge by a factor of 2 after each transformation, is truncated after $\ln(L/2a)/\ln(2)$ iterations so that an $L \times L \times L$ cluster with fraction p of $\epsilon_m(\omega)$ bonds is reduced to a single effective cluster of dielectric $\epsilon(p, \omega)$.

Figure 3(a) shows our results for $\ln[\epsilon'(p, \omega)]$ and $\ln[\epsilon''(p, \omega)]$ versus p , for clusters of sizes $L/2a = 2^3, 2^4, 2^5$, respectively, and at a frequency corresponding to 1 meV. The metal dielectric function is again assumed describable by a Drude model with an electron relaxation time $\tau = a^*/v_f$ where a^* is an effective radius which represents a contact resistance between connected metal particles. The host dielectric constant ϵ_b has contributions from the impurity- and/or oxide-coated metal particles and is taken to be a constant, here $\epsilon_b = 10$. Contributions to the absorption from the coated metal component are negligible and may be neglected. The metal is Sn with $\omega_p = 1.17 \times 10^{16} \text{ sec}^{-1}$, $v_f = 1.24 \times 10^8 \text{ cm/sec}$, $a = 250$ Å, and $a^* = 80$ Å. At large fill fractions, $p \geq 0.30$, all cluster sizes exhibit similar behavior in $\epsilon''(p, \omega)$. However, near $p_c = 0.208$ of the infinite system, the larger clusters show a sharper behavior in $\epsilon''(p, \omega)$ [see Fig. 3(a)]. The sudden decrease in $\epsilon'(p, \omega)$ at high p is due to the increasing contribution of $\text{Re}\epsilon_m(\omega) \ll 0$ to $\epsilon'(p, \omega)$.

Figures 3(b) and 3(c) show $\ln[\epsilon'(p, \omega)]$ and $\ln[\epsilon''(p, \omega)]$ versus p for $L/2a = 2^3, 2^4$ at frequencies corresponding to 1, 2, and 4 meV. At large p all the clusters exhibit metallic behavior, that is, $\epsilon''(p, \omega) \approx 1/\omega$. In the transition region the metallic behavior is slowly lost and at sufficiently small p , $\epsilon''(p, \omega) \approx \omega$, which reflects the response of the isolated particles only. The crossover from dielectric to metallic behavior depends crucially on cluster size, as the smaller clusters are predominantly metallic over the entire range of fill fractions considered. However, all clusters

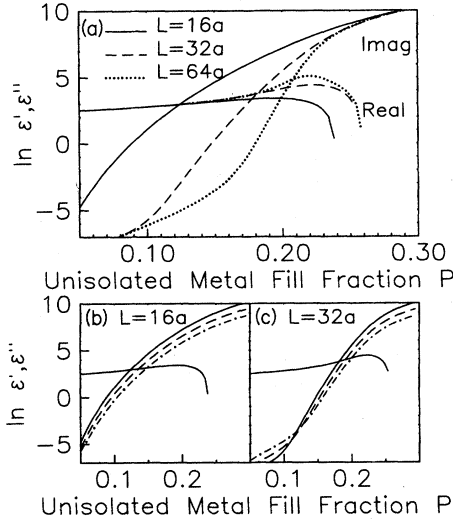


FIG. 3. Cluster dielectric functions used in cluster percolation model: $\ln[\epsilon'(p,\omega)]$, $\ln[\epsilon''(p,\omega)]$ vs p and ω as calculated via a renormalization-group technique for a lattice model of a cluster with a fraction p of metal particles able to have metallic contact with neighbor particles. The metal particles of radius a are assumed describable by a dielectric function of the Drude form with $\tau \approx a/v_f$. (a) $\ln \epsilon'$, $\ln \epsilon''$ vs p for various clusters sizes at fixed frequency. The slope of $\ln \epsilon''$ increases with increasing cluster size for p near the percolation threshold $p_c \approx 0.208$ of an infinite system of perfect conductors in a nonconducting host. (b) $\ln \epsilon'$, $\ln \epsilon''$ for $L=16a$ cluster at 1 meV (solid line), 2 meV (dashed line), and 4 meV (dash-dot line). $\epsilon'' \approx 1/\omega$, indicating metallic behavior, for all p shown while ϵ' is independent of frequency in this range of p . (c) As in (b) with $L=32a$. For this larger cluster, ϵ'' shows a turnover to $\approx \omega$, indicating insulating behavior, at low p .

must be insulating at $p=0$.

The absorption of an isolated cluster is determined by the imaginary part of its polarizability, that is,

$$\alpha_{\text{cluster}} \approx \frac{\epsilon''(p,\omega)}{\epsilon'(p,\omega)^2 + \epsilon''(p,\omega)^2}. \quad (3.1)$$

Clusters contributing most to the absorption at a frequency ω are clearly those which have unisolated metal fill fractions near a p_m satisfying $\epsilon'(p_m,\omega) = \epsilon''(p_m,\omega)$. As apparent from Fig. 3, the clusters of interest for absorption in the FIR region are thus the clusters with metal fill fractions p near the transition region. We must therefore be concerned with how well a lattice model and RG calculation of $\epsilon(p,\omega)$ for the finite system represents the correct, average dielectric function near the percolation region. The magnitude of the absorption depends primarily on the magnitude of $\epsilon(p_m,\omega)$, a quantity which is fairly insensitive to the calculational technique. However, as will be evident in the next section the frequency dependence of the composite absorption actually depends on how rapidly the slope of $\epsilon''(p,\omega)$ changes as a function of frequency for p near p_m . In turn, this slope depends strongly on the cluster size and calculation technique.

Accordingly, we caution that the frequency dependence of α , as calculated in the following section using $\epsilon(p,\omega)$ calculated here, may not be an accurate representation of the frequency dependence of the true composite $\alpha(\omega)$.

B. Composite dielectric function and absorption coefficient

The clusters for which $\epsilon(p,\omega)$ was calculated in the previous section are assumed to be uniform in size and much smaller than the wavelength λ of the incident radiation, $R \ll \lambda$; the quasistatic limit is thus obtained. In addition, since the total metal fill fraction is $f \ll 1$, the fill fraction of each "bin" of clusters is also small, namely $fN(p)dp \ll 1$, independent of the "bin" size dp . Within these limits, the multicomponent Maxwell-Garnett dielectric function for a dilute collection of spherical inclusions is applicable, and leads to

$$\epsilon_{\text{comp}}(\omega) = \epsilon_h \left[1 + 3f \int dp N(p) \frac{\epsilon(p,\omega) - \epsilon_h}{\epsilon(p,\omega) + 2\epsilon_h} \right], \quad (3.2)$$

where ϵ_h is the host dielectric constant. In the small- f limit, the MG result numerically is equivalent to an effective dielectric function calculated for an aggregate topology (e.g., the Bruggeman or effective medium theories¹³). Once again, the absorption coefficient is calculated from $\alpha(\omega) = (2\omega/c) \text{Im} \epsilon(\omega)^{1/2}$.

The distribution function $N(p)$ is not explicitly known. However, on general grounds the close random-packing fraction of $p_{\text{max}} \approx 0.65$ must provide an upper limit to $N(p)$. While $N(p)$ does depend on the way in which the cluster formation process proceeds and also on the relative probabilities of finding isolated and unisolated metal particles in a cluster, we expect $N(p)$ to be relatively featureless over the scale of the substantial variations in the dielectric function $\epsilon(p,\omega)$. By way of example, we have chosen $N(p)$ to be a constant over $0 < p < 0.30$ and zero elsewhere so that $\alpha(\omega)$ and $\epsilon_{\text{comp}}(\omega)$ will reflect the inherent structure in $\epsilon(p,\omega)$ and the cluster polarizability. This choice of $N(p)$ provides merely an overall scale factor for the absorption and does not influence the frequency dependence of the composite absorption.

The absorption coefficient versus frequency as calculated by Eq. (3.2) using $\epsilon(p,\omega)$ as shown in Fig. 3(b) is presented in Fig. 4. The parameters $f=0.02$ and $\epsilon_h=4.84$ were chosen to correspond to the oxide-free samples studied by Curtin *et al.* The cluster radius is thus $R \approx 8a = 2000 \text{ \AA}$. We note that the magnitude of the absorption at low frequencies is again quite large: $\alpha(1 \text{ meV} \equiv 8 \text{ cm}^{-1}) = 0.49 \text{ cm}^{-1}$, which, remarkably, is within a factor of 3 of the experimental value. The magnitude of α is fairly insensitive to the magnitude of the metallic component dielectric function but is roughly proportional to $\epsilon_b^{-1/2}$. The frequency dependence is very nearly linear (in some disagreement, it should be noted, with the oxide-free sample results) but may be easily understood in that at all frequencies considered the real and imaginary parts of $\epsilon(p,\omega)$ intersect at nearly the same value and with nearly the same slope. The imaginary part of the integral in Eq. (3.2) is thus a weak function of ω and the frequency dependence of α is controlled by the ω prefactor.

The absorption coefficient versus frequency for the

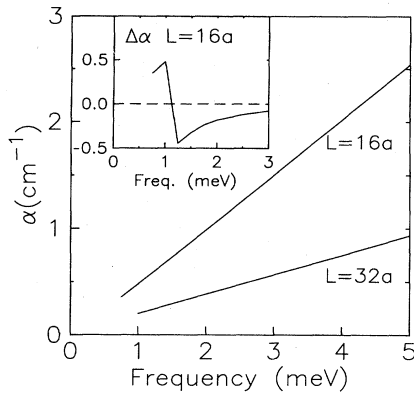


FIG. 4. Absorption coefficient $\alpha(\omega)$ vs ω for cluster percolation model at cluster sizes of $L=16a=4000 \text{ \AA}$ and $L=32a=8000 \text{ \AA}$. The cluster dielectric functions are as shown in Figs. 3(b) and 3(c), respectively. The parameters are chosen to correspond to the oxide-free samples studied in Ref. 11: metal fill fraction $f=0.02$, particle radius $a=250 \text{ \AA}$, and host dielectric $\epsilon_h=4.84$. The absorption is large and nearly linear in frequency. Inset— $\Delta\alpha$ for $L=16a$. Above the superconducting gap frequency $\Delta\alpha$ is negative, has a minimum near $\omega \approx 1.25\omega_g$, and decreases toward zero at higher frequencies, as is seen experimentally.

larger clusters $R=16a$ as calculated by Eq. (3.2) with $\epsilon(p,\omega)$ as in Fig. 3(c) is also presented in Fig. 4. The absorption coefficient is again large in magnitude although smaller than that obtained for the smaller clusters and again α is fairly insensitive to variations in $\epsilon_m(\omega)$. The frequency dependence is also approximately linear. A stronger frequency dependence may be obtained, at a cost of lower magnitude, by assuming the isolated metallic inclusions to be more polarizable, thereby increasing ϵ_b . Calculations of α versus ω for $\epsilon_b=50$ and 100 yield frequency dependences of $\omega^{1.33}$ and $\omega^{1.47}$, with magnitudes reduced by factors of 4.1 and 6.4 relative to the $\epsilon_b=10$ results, respectively. However, the $L/2a=2^4$ cluster calculations for $a=250 \text{ \AA}$ correspond to a cluster of radius $R=4000 \text{ \AA}$ which is larger than expected to be found experimentally.

The composite absorption coefficient in the superconducting state may be calculated in the same way as that of the normal state with the use of the MB dielectric function for the superconducting metallic component. The difference absorption, $\Delta\alpha$, shown in the inset of Fig. 4 exhibits a positive peak near ω_g and a negative peak at a higher frequency followed by a decrease in $\Delta\alpha$ to zero at very high frequencies, $\omega \gg \omega_g$. The calculated $\Delta\alpha$ is consistent with experimental observations but since the normal absorption as calculated differs from experiment, no quantitative agreement in $\Delta\alpha$ should be expected.

The cluster percolation model predicts absorption coefficients comparable to those measured at low frequencies and also predicts a $\Delta\alpha$ with the same general characteristics as those observed. However, the frequency dependence of α within the model deviates considerably from the near-quadratic behavior usually observed. The discrepancy may be primarily a result of the lattice-model

RG technique employed to calculate $\epsilon(p,\omega)$. We expect the frequency dependence of α to be between ω and ω^2 for any type of calculation of $\epsilon(p,\omega)$ while the magnitude of α should remain comparable to experimental values at low frequencies.

IV. CLUSTER TUNNEL JUNCTION MODEL

The final structural model we consider for FIR absorption is the cluster tunnel junction model. This model assumes that the metal particles in a cluster are electrically coupled to their neighbors but only by tunnel junctions. Absorption then occurs in the clusters by means of photon-assisted tunneling of electrons between particles. Each cluster is modeled as a cubic array of identical metal particles of radius a with nearest-neighbor separations of $2a+t$. Each particle is considered to have a dc resistivity ρ_m while each tunnel junction (of area A and width t) is modeled by a frequency-independent resistivity ρ_J in parallel with a capacitance C_J .¹⁸ Elementary circuit analysis then shows that the effective complex resistivity of the cluster along any cube axis is simply

$$\rho_{\text{eff}} = \rho_m + \rho_J \frac{2at}{A} (1 - i\omega C_J \rho_J t / A)^{-1}, \quad (4.1)$$

where γ is a geometrical factor and depends on the lattice structure. For a good metallic component, ρ_m may be neglected and the cluster dielectric function becomes

$$\epsilon_{\text{eff}} = \frac{4\pi i}{\omega \rho_{\text{eff}}} = \frac{2\pi\gamma}{a} (C_J + iA/\omega\rho_J t). \quad (4.2)$$

The composite consists of a fill fraction $\eta \ll 1$ of identical clusters described by ϵ_{eff} . The composite dielectric function is calculated using the MG form and leads to

$$\epsilon_{\text{comp}} = \epsilon_h \left[1 + 3\eta \frac{\epsilon_{\text{eff}} - \epsilon_h}{\epsilon_{\text{eff}} + 2\epsilon_h} \right]. \quad (4.3)$$

Negligible geometric effects are expected from the use of (4.3), appropriate to spherical inclusion, and (4.2), appropriate to cubic arrays. The absorption coefficient for the composite is thus

$$\alpha(\omega) = \frac{9}{4\pi\gamma} \epsilon_h^{3/2} \eta \frac{\omega^2}{c} \frac{\sigma_J A / 2at}{(C_J 2a + \epsilon_b / 2\pi)^2 \omega^2 + (\sigma_J A / 2at)^2}. \quad (4.4)$$

At sufficiently low frequencies, the interparticle tunneling conductivity dominates the capacitive coupling and the absorption is quadratic in frequency and proportional to σ_J^{-1} . As the frequency increases, capacitive coupling becomes increasingly important and the absorption begins to saturate. The onset of noticeable saturation occurs as $C_J \omega$ approaches $A\sigma_J/t$.

To determine the absorption coefficient, we have calculated σ_J , the single-junction conductivity, within a simple step potential-barrier model. In the limit $\omega \ll \omega_p$ and with a barrier height V_0 we find

$$\sigma_J = \left[\frac{e^2 k_f}{\hbar} \right] \frac{k_f t}{\beta^2 \pi^2} e^{-2\beta t}, \quad (4.5)$$

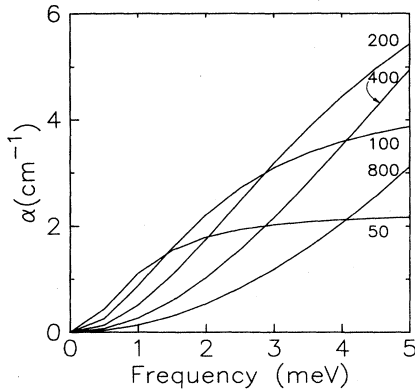


FIG. 5. Absorption coefficient $\alpha(\omega)$ vs ω for cluster tunnel junction model for various junction conductivities in $(\Omega \text{ cm}^{-1})^{-1}$. The absorption is large and is quadratic in ω at low frequencies if charging energies are small enough to be neglected.

where $\beta = [(V_0 - E_F)2m/\hbar^2]^{1/2}$ and E_F is the Fermi energy. We have also calculated C_J by the method of images for pairs of spherical particles of radius a separated by a distance $2a + t$ and embedded in dielectric ϵ_b for relevant values of a , t , and ϵ_b . We estimate the tunneling area between two spheres as $A = \pi a / \beta$. Lastly, η is related to the metallic fill fraction f by $\eta = f / f_c$ where f_c is the appropriate cubic lattice close-packed ratio.

Shown in Fig. 5 is $\alpha(\omega)$ versus ω as calculated from Eq. (4.4) for a bcc lattice, $a = 250 \text{ \AA}$, $t = 5 \text{ \AA}$, $\beta = 0.70 \text{ \AA}^{-1}$, $f = 0.02$, $\epsilon_b = 5.0$, $C_J = 2000 \text{ \AA}$, and $\sigma_J = 50, 100, 200, 400$, and $800 (\Omega \text{ cm}^{-1})^{-1}$. Here $\sigma_J = 100 (\Omega \text{ cm}^{-1})^{-1}$ corresponds to the value calculated via Eq. (3.5). The magnitude of α is again large for this range of junction conductivities. In addition, the frequency dependence is quadratic at low frequencies and significant deviations at higher frequencies are only evident for the lower values of σ_J . While the conductivities as given by Eq. (4.5) can seemingly vary over a very wide range, the values we use here are actually quite comparable to tunneling conductivities estimated from studies of electrical transport in granular composites.¹⁹ The interparticle resistance for $\sigma_J = 200 (\Omega \text{ cm}^{-1})^{-1}$ is $R_J \approx 2000 \Omega$. The absorption coefficient depends only weakly on the particle size since σ_J is size independent (for particles where quantum size effects are not important) and since C_J/a is also weakly size dependent.

In calculating the junction conductivity σ_J [Eq. (4.5)] we have not yet accounted for the finite charging energy E_c required to create a charged pair of neighboring particles. The inclusion of a charging energy leads immediately to an activated junction conductivity.²⁰ At $T = 0$ tunneling can only occur if $\hbar\omega > E_c$ and at finite temperatures (on the order $kT = E_c = \hbar\omega$) the junction conductivity is therefore a strong function of temperature and frequency. Since no temperature dependence is observed in experimental studies of α between 4 and 27 K, the cluster tunnel junction model is physically acceptable only if $E_c \ll \hbar\omega$ over the experimental range of frequencies. We may readily estimate E_c for the cubic lattice model used here. The charging energy is related to the total capaci-

TABLE I. Charging energy E_c required to transfer a single electron between two neighboring metal particles, of radii a and center-to-center separation $2a + t$, embedded in a cubic lattice having z identical nearest-neighbor particles and a background dielectric constant ϵ_b .

$a (a_0)$	$t (a_0)$	z	$\bar{C}_J (a_0)$	ϵ_b	E_c (MeV)
475	10	8	758	5	0.90
475	10	12	758	5	0.60
100	10	8	130	5	5.2
100	10	8	130	10	2.6
100	10	12	130	10	1.7

tance C between two neighboring particles by $E_c = e^2 / 2C$. The total capacitance C is related to the single-junction capacitance by $C = zC_J / 2$, z being the coordinate number of lattice (assumed infinite in extent). Note that we can write $C_J = \bar{C}_J \epsilon_b$ to scale out the background dielectric constant. Table I presents estimates of E_c for various parameter values. The estimates of E_c for the larger particles are on the borderline since the minimum experimental frequencies are near $8 \text{ cm}^{-1} \equiv 1 \text{ meV}$. For the much smaller particles ($a = 50 \text{ \AA}$), E_c appears to be fairly large; it is certainly not negligible. However, our estimate is based on a neutral system with only a single charge pair present. If local defects or impurities shift the local potentials slightly, it is plausible that some pair charging energies will be lower than our estimates and that thermal excitation of these pairs will change many other pair charging energies to lower values. Values of $E_c < 0.25 \text{ meV}$ are necessary, however, for the temperature dependence of α to be negligible.

Lastly, we remark that the CTJ model should give qualitatively the correct superconducting absorption and $\Delta\alpha$. Below ω_g , the superconducting tunnel conductivity $\sigma_J(\text{SC})$ is zero and thus $\alpha_s = 0$ and $\Delta\alpha = \alpha_n$. At ω_g , the junction conductivity increases discontinuously. BCS theory predicts that $\sigma_J(\text{SC}) = 3\sigma_J(n)/4$ at the gap. Since α is inversely dependent on σ_J we expect $\Delta\alpha = -\alpha_n/3$ at the gap when capacitive effects are small. As ω increases beyond ω_g , $\sigma_J(\text{SC})$ approaches $\sigma_J(n)$ rapidly and $\Delta\alpha$ should go to zero.

The CTJ model also predicts absorption coefficients agreeing in magnitude, frequency dependence, and $\Delta\alpha$ with experimental observations, but only under the assumption of sufficiently small charging energies. Although the effects of disorder in the junction positions and variations in the junction conductivities have not been considered, the encouraging results found in our simple model suggest that tunneling within clusters is a possible mechanism for FIR absorption in metal-insulator composites.

V. DISCUSSION

Since most experimental and theoretical studies find that α is linear in the total metal fill fraction f , it is useful for comparison purposes to consider the quantity $\alpha(\omega)/f$ at a fixed frequency. At $1 \text{ meV} \equiv 8 \text{ cm}^{-1}$, the typical experimental values are in the range $\alpha(8 \text{ cm}^{-1})/f = 5-50$.

TABLE II. Comparison between experimental values and various theoretically calculated values of $\alpha(8 \text{ cm}^{-1})/f$ for particles of radius 250 \AA . The three models presented here predict absorption coefficients quite comparable in magnitude to the experimental values while all previous theories fail to attain the necessary magnitude. The theories have been presented in order of decreasing absorption coefficient.

Theory	$\alpha(8 \text{ cm}^{-1})/f$ (cm^{-1})
(Experiment)	5–50
Fused cluster	5–35
Cluster percolation	5–25
Cluster tunnel junction	5–25
Needle clusters, coated (Refs. 6, 8, and 9)	2
Coated sphere (Ref. 6)	0.3–3
Surface phonon (Ref. 4)	0.4
Single-particle magnetic dipole (Refs. 13 and 15)	0.2
Single-particle, nonlocal (Ref. 5)	0.004
Single-particle electric dipole (Ref. 15)	0.004

Table II shows this quantity for 250 \AA particles both for our theories and for previous theories. The three models we have introduced lead to absorption that is considerably enhanced relative to classical single-particle theories. The physical origins of this enhancement are the following: In magnetic dipole theory the absorption depends strongly on size. Accordingly, the fused-cluster-model absorption introduces a factor of nearly $(R/a)^2$ relative to the single-metal-particle MD absorption. In the electric dipole theory, the absorption depends on the real and imaginary components of the dielectric function ϵ through a quantity $\approx \epsilon''/(\epsilon'^2 + \epsilon''^2)$. Both the cluster percolation and CTJ models have very poorly conducting clusters in comparison to that of the metallic components (i.e., $\epsilon'' \ll \epsilon''_{\text{metal}}$) leading in each case to an enhancement of roughly $\epsilon''_{\text{metal}}/\epsilon''$ over the single-metal-particle ED absorption.

We also note that the presence of oxide coating deliberately placed on the particles in some samples is likely to prevent a transition of all clusters to the fully fused state. In this case, the heat-treated sample α_n and $\Delta\alpha$ would be attributable almost equally to features from a

combination of the CP and/or CTJ models, and the FC model. We expect from the similarities between Figs. 2, 4, and 5 that α_n would show negligible changes on heating but that $\Delta\alpha$ would have canceling contributions [compare Figs. 2 (inset) and 4 (inset)] and be fairly featureless above ω_g . These expectations are consistent with the experimental observations on the oxide samples studied by Curtin *et al.*

The models used here to describe unheated clusters are simple lattice models which do not take into account in detail the randomness in the positions of the metal particles within a cluster. In addition, our calculations have been carried out on very symmetric model clusters, i.e., spheres and cubes, and although geometrical effects associated with shape distortions and elongations are expected to have only minor effects on the general results we have presented, they have not been considered. Further theoretical efforts should be made to include these aspects and to improve on the calculations of $\epsilon(p, \omega)$ in the CP model, if possible. Nevertheless, the general success in describing all the absorption coefficient features, particularly the magnitude, within physically reasonable and realizable assumptions is unmatched to data. This success is further strengthened by the topological consistency between models, that is, both the CP and CTJ models have clusters with limited interparticle metallic contact. Upon heating, the metal components fuse and break the nonconducting barriers, leading to the topology of the FC model. Further, the CP and CTJ models are also *not* mutually exclusive. Hence, the unheated composite might well have absorption contributions from clusters of the CP topology, from the CTJ topology, or from clusters which allow both tunneling and some metallic contact simultaneously.

Since our results indicate that the electromagnetic response in these composite systems is dominated by large clusters composed of particles which differ little from bulk metal, future experiments should be directed toward the study of much smaller sized, well-dispersed particles in the hope of observing the interesting size effects which have been predicted by previous theories.^{4,5,7}

ACKNOWLEDGMENTS

We would like to thank R. C. Spitzer and Professor A. J. Sievers for advice and continued interest in this work. We also wish to thank Dr. S. Solla and J. Mantese for many helpful discussions. This work was supported by the National Science Foundation through the Materials Science Center at Cornell University (Grant No. DMR-8217227a-01, MSC Report No. 5438).

¹D. B. Tanner, A. J. Sievers, and R. A. Buhrman, Phys. Rev. B **11**, 1330 (1975).

²G. L. Carr, R. L. Henry, N. E. Russell, J. C. Garland, and D. B. Tanner, Phys. Rev. B **24**, 777 (1981).

³G. Mie, Ann. Phys. (N.Y.) **25**, 377 (1908).

⁴A. J. Glick and E. D. Yorke, Phys. Rev. B **18**, 2490 (1978).

⁵P. Apell, Phys. Scr. **29**, 146 (1984).

⁶P. N. Sen and D. B. Tanner, Phys. Rev. B **26**, 3582 (1982).

⁷D. M. Wood and N. W. Ashcroft, Phys. Rev. B **25**, 6255 (1982).

⁸E. Simanek, Phys. Rev. Lett. **38**, 1161 (1977).

⁹R. Rupp, Phys. Rev. B **19**, 1318 (1979).

¹⁰G. L. Carr, J. C. Garland, and D. B. Tanner, Phys. Rev. Lett. **50**, 1607 (1983).

- ¹¹W. A. Curtin, R. C. Spitzer, N. W. Ashcroft, and A. J. Sievers, Phys. Rev. Lett. (to be published).
- ¹²R. P. Devaty and A. J. Sievers, Phys. Rev. Lett. **52**, 1344 (1984).
- ¹³D. Stroud and F. P. Pan, Phys. Rev. B **17**, 1602 (1978).
- ¹⁴Petr Chýlek and Vandana Srivastava, Phys. Rev. B **27**, 5098 (1983). See, however, the comment on this paper by D. B. Tanner, Phys. Rev. B **30**, 1042 (1984) and the revisions contained in Petr Chýlek and Vandana Srivastava, *ibid.* **30**, 1008 (1984).
- ¹⁵J. C. Maxwell-Garnett, Philos. Trans. R. Soc. London **203**, 385 (1904).
- ¹⁶D. C. Mattis and J. Bardeen, Phys. Rev. **111**, 412 (1958).
- ¹⁷J. Bernasconi, Phys. Rev. B **18**, 2185 (1978); and S. Solla (unpublished).
- ¹⁸The results of this type of model are similar to those for absorbing oxide-coated sphere models. Here the junction plays the role of the poorly conducting coating. See Ref. 6 for comparison.
- ¹⁹R. Laibowitz, A. Broers, D. Stroud, and B. R. Patton, in *Inhomogeneous Superconductors*, edited by D. U. Gubser, T. L. Francavilla, J. R. Leibowitz, and S. A. Wolf (American Institute of Physics, New York, 1979), p. 263.
- ²⁰B. Abeles, Ping Sheng, M. D. Coutts, and Y. Arie, Adv. Phys. **24**, 407 (1975).